

2003

# Anisotropy and large magnetoresistance in the narrow-gap semiconductor FeSb<sub>2</sub>

Cedomir Petrovic  
*Iowa State University*

J.W. Kim  
*Iowa State University*

Sergey L. Bud'ko  
*Iowa State University, budko@ameslab.gov*

A. I. Goldman  
*Iowa State University, goldman@ameslab.gov*

Paul C. Canfield  
*Iowa State University, canfield@ameslab.gov*

Follow this and additional works at: [http://lib.dr.iastate.edu/chem\\_pubs](http://lib.dr.iastate.edu/chem_pubs)

 Part of the [Biological and Chemical Physics Commons](#), [Materials Chemistry Commons](#), [Other Chemistry Commons](#), and the [Physical Chemistry Commons](#)

The complete bibliographic information for this item can be found at [http://lib.dr.iastate.edu/chem\\_pubs/843](http://lib.dr.iastate.edu/chem_pubs/843). For information on how to cite this item, please visit <http://lib.dr.iastate.edu/howtocite.html>.

---

# Anisotropy and large magnetoresistance in the narrow-gap semiconductor FeSb<sub>2</sub>

## Abstract

A study of the anisotropy in magnetic, transport, and magnetotransport properties of FeSb<sub>2</sub> has been made on large single crystals grown from Sb flux. Magnetic susceptibility of FeSb<sub>2</sub> shows diamagnetic to paramagnetic crossover around 100 K. Electrical transport along two axes is semiconducting, whereas the third axis exhibits a metal-semiconductor crossover at temperature  $T_{cr}$  which is sensitive to current alignment and ranges between 40 and 80 K. In  $H=70\text{kOe}$  semiconducting transport is restored for  $T<300\text{K}$ , resulting in large magnetoresistance  $[\rho(70\text{kOe})-\rho(0)]/\rho(0)=2200\%$  in the crossover temperature range.

## Disciplines

Biological and Chemical Physics | Materials Chemistry | Other Chemistry | Physical Chemistry

## Comments

This article is from *Physical Review B* 67 (2003): 1, doi:[10.1103/PhysRevB.67.155205](https://doi.org/10.1103/PhysRevB.67.155205). Posted with permission.

## Authors

Cedomir Petrovic, J.W. Kim, Sergey L. Bud'ko, A. I. Goldman, Paul C. Canfield, Wonyoung Choe, and Gordon J. Miller

**Anisotropy and large magnetoresistance in the narrow-gap semiconductor FeSb<sub>2</sub>**

C. Petrovic,\* J. W. Kim, S. L. Bud'ko, A. I. Goldman, and P. C. Canfield

*Ames Laboratory and Department of Physics and Astronomy, Iowa State University, Ames, Iowa 50011*

W. Choe and G. J. Miller

*Ames Laboratory and Department of Chemistry, Iowa State University, Ames, Iowa 50011*

(Received 11 June 2002; revised manuscript received 20 December 2002; published 14 April 2003)

A study of the anisotropy in magnetic, transport, and magnetotransport properties of FeSb<sub>2</sub> has been made on large single crystals grown from Sb flux. Magnetic susceptibility of FeSb<sub>2</sub> shows diamagnetic to paramagnetic crossover around 100 K. Electrical transport along two axes is semiconducting, whereas the third axis exhibits a metal-semiconductor crossover at temperature  $T_{cr}$  which is sensitive to current alignment and ranges between 40 and 80 K. In  $H=70$  kOe semiconducting transport is restored for  $T<300$  K, resulting in large magnetoresistance  $[\rho(70 \text{ kOe})-\rho(0)]/\rho(0)=2200\%$  in the crossover temperature range.

DOI: 10.1103/PhysRevB.67.155205

PACS number(s): 72.20.-i, 75.20.-g, 73.63.-b

Small gap semiconductors are materials of choice not only as model electronic systems in materials physics but also in many applications. Semiconducting compounds often show many phenomena not seen in pure silicon, such as a variety of optical effects and giant magnetoresistance. Ultimately, they can be rather flexible in material design due to the possibility for tuning their fundamental physical properties. Highly anisotropic semiconductors with directional bands and low dimensional conducting states can provide an important bridge between bulk and mesoscopic semiconducting materials. One such material is FeSb<sub>2</sub>.<sup>1</sup> It represents an interesting case of a semiconductor where a band of itinerant electron states originates in the  $d_{xy}$  orbitals of the  $t_{2g}$  multiplet, which overlap along the  $c$  axis of the crystal, distinguishing its loengillate crystal structure from normal marcasites.<sup>2,3</sup> Its magnetic susceptibility is reminiscent of the one seen in another narrow gap semiconductor FeSi but with a very small low temperature impurity tail in the diamagnetic region.<sup>4</sup> In this work, we examine the anisotropic magnetic and electronic properties of FeSb<sub>2</sub>, discuss the possible mechanism for these phenomena, and suggest pathways for further theoretical and experimental work.

Synthesis of large single crystals of FeSb<sub>2</sub> has allowed us to study the anisotropy in its magnetic and electrical transport properties. The self-flux method of crystal growth is particularly convenient for the growth of semiconducting compounds, since it does not introduce any additional elements into the melt which could randomly fill the band structure with impurity states.<sup>5-7</sup> To this end, single crystals of FeSb<sub>2</sub> were grown from an initial composition of constituents Fe<sub>0.08</sub>Sb<sub>0.92</sub>. The constituent elements were placed in an alumina crucible and sealed in a quartz ampoule. After initial heating to 1000 °C, the melt was fast cooled to 800 °C in 14 h, then slow cooled to 650 °C where excess Sb flux was removed via decanting. The crystals grew as silvery rods, their long axis parallel to the  $b$  crystalline axis.

Room temperature (around 300 K) x-ray diffraction data of a single crystal of FeSb<sub>2</sub> were collected using a Bruker CCD-1000 diffractometer with Mo  $K_{\alpha}$  radiation ( $\lambda=0.71073$  Å). The structure solution was obtained by direct methods and refined by a full-matrix least-squares refinement

of  $F_0^2$  using the SHELXTL 5.12 package. Powder x-ray diffraction spectra are taken with Cu  $K_{\alpha}$  radiation in a Scintag diffractometer. Electrical contacts were made with Epotek H20E silver epoxy. Several different single crystals were oriented by a Laue camera and were cut in a rectangular shape along each crystal axis. Their resistivity was measured by LR 700 resistance bridge from 1.8 to 300 K and in fields up to 70 kOe. These measurements, as well as magnetic measurements, have been performed in the  $H,T$  environment of Quantum Design MPMS-5 and MPMS-7 magnetometers. Magnetic susceptibility was measured by mounting oriented sample on a disk whose background has been subtracted, in a typical field of 50 kOe.

FeSb<sub>2</sub> crystallizes into a marcasite structure similar to rutile (TiO<sub>2</sub>), a structure observed primarily for oxides, for example, VO<sub>2</sub> (Fig. 1). Basic construction units in both structures are TiO<sub>6</sub> (FeSb<sub>6</sub>) octahedra that form edge sharing chains along the  $c$  axis, sharing corners between chains. The tilt of octahedra in the  $ab$  plane orthogonal to chain direction

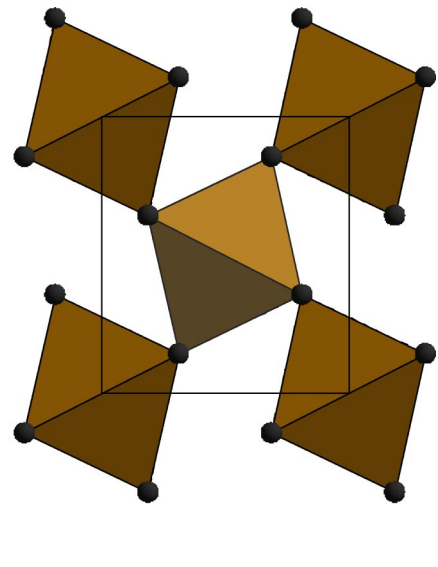


FIG. 1. Crystal structure of FeSb<sub>2</sub> showing Fe surrounded by Sb octahedra.

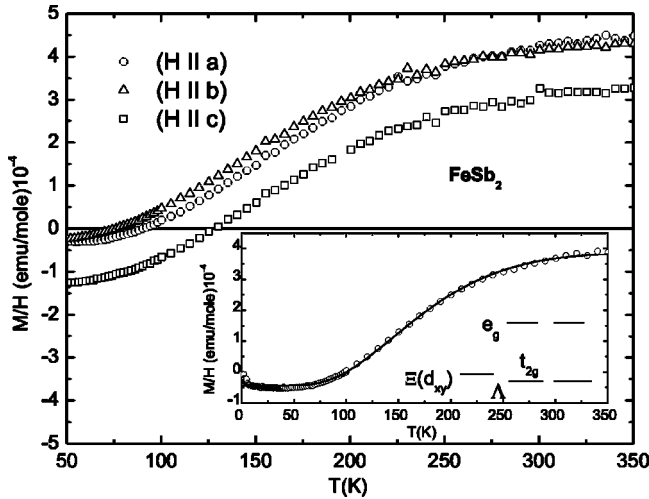


FIG. 2. Magnetic susceptibility of FeSb<sub>2</sub> single crystal grown by the flux method. Inset: fit of polycrystalline susceptibility for low spin to high spin transition. Open circles represent data taken on different samples. The solid line is fit to a model of low to high spin transition (see text).

distinguishes the marcasite structure from rutile.

Since phase purity and questions of exact stoichiometry are important in semiconductor physics, we performed a thorough structural analysis. A crystal with dimensions 0.25 × 0.19 × 0.13 mm<sup>3</sup> was chosen for the data set collection. The space groups corresponding to the observed systematic extinctions are the orthorhombic groups *Pnmm* and *Pnn2*. We refined the structure in the *Pnmm*, the centrosymmetric space group of the two. Lowering symmetry from *Pnmm* to *Pnn2* led to no meaningful decrease in *R* factor. Crystallographic data taken on single crystal of FeSb<sub>2</sub> are in accordance with previously reported data, and consistent with the orthorhombic marcasite structure with lattice constants *a* = 5.815(4), *b* = 6.517(5), and *c* = 3.190(2) Å.<sup>8</sup> Single crystal x-ray diffraction measurement showed that site occupancy does not deviate from an ideal FeSb<sub>2</sub> stoichiometry to within our 1% resolution limit. In addition to this, powder x-ray pattern taken on several randomly chosen samples grown under the same conditions was consistent with the FeSb<sub>2</sub> structure with no additional impurity phases present.

Figure 2 shows magnetic susceptibility of the FeSb<sub>2</sub> measured along the *a*, *b* and *c* axes of the crystal. It is qualitatively similar to the polycrystalline magnetic susceptibility obtained on crystals grown by a vapor transport technique.<sup>9</sup> All three directions have similar temperature dependences but for *H*||*c* there is a shift of  $\sim -1 \times 10^{-4}$  emu/mole. The polycrystalline magnetic susceptibility directly measured on different sample can be estimated by  $\chi_{\text{poly}} = \frac{1}{3}(\chi_a + \chi_b + \chi_c)$  and is shown in the inset of Fig. 2. It increases with an increase in temperature from a low temperature diamagnetic and temperature independent value of  $-4 \times 10^{-5}$  emu/mole (close to the core diamagnetism value of  $-4.7 \times 10^{-5}$ ), passes through a region of diamagnetic to paramagnetic crossover and becomes paramagnetic at high temperatures. The crossover temperatures are  $\sim 100$  K for the field applied along the *a* and *b* axes and  $\sim 125$  K for the field applied along the *c* axis.

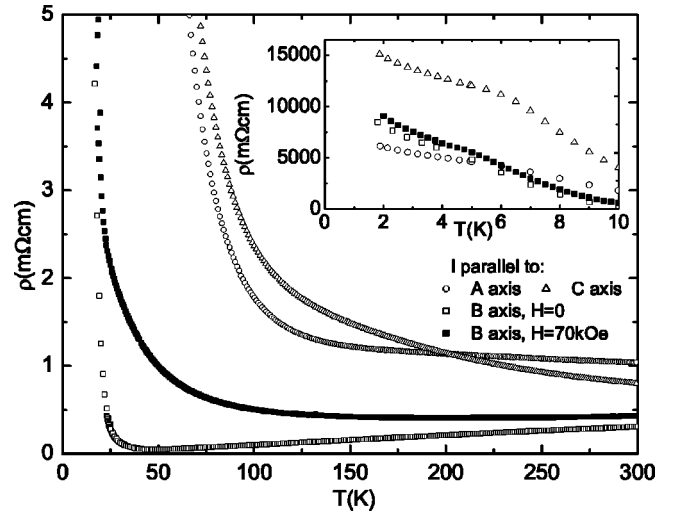


FIG. 3. Anisotropy in electrical transport of FeSb<sub>2</sub>. The inset shows low temperature resistivity with a clear contribution of impurity states below 5 K.

Whereas the anisotropy in  $\chi(T)$  of FeSb<sub>2</sub> is relatively small, the anisotropy in the electrical resistivity  $\rho(T)$  is dramatic (Fig. 3). For the current along either the *a* and *c* axis,  $\rho(T)$  is semiconducting over the entire temperature range. The resistivity increases by four orders of magnitude down to the lowest measured temperature of 1.8 K [Fig. 3 (inset)]. From arrhenius plots of  $\rho(T)$  curves we can estimate gap values  $\Delta_{\rho}(a,c) \approx 300$  K [Fig. 4 (inset)], in accordance with previous results.<sup>9</sup>

The *b* axis transport manifests a metallic behavior above  $\sim 40$  K, with a resistivity ratio (RR) =  $\rho(300 \text{ K})/\rho(40 \text{ K}) = 6.3$  (extrapolation to *T*=0 of the high-temperature *b* axis resistivity gives RR=98). Below 40 K the *b*-axis resistivity increases five orders of magnitude, to values comparable to the *a* and *c* axes resistivity, and shows activated behavior only below *T*<sub>min</sub> ( $\sim 40$  K for optimal current orientation)

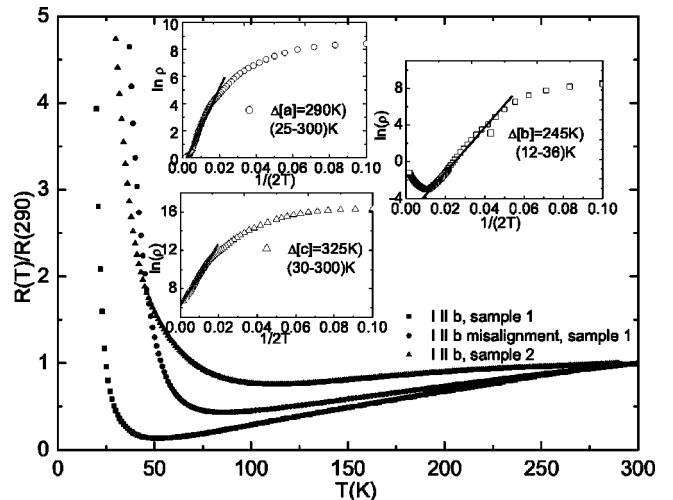


FIG. 4. Crossover temperature region of *b*-axis electrical transport. Note the substantial influence of deliberate current misalignment in the *ab* plane for sample 1. The inset shows activated behavior of resistivity for all three crystallographic directions.

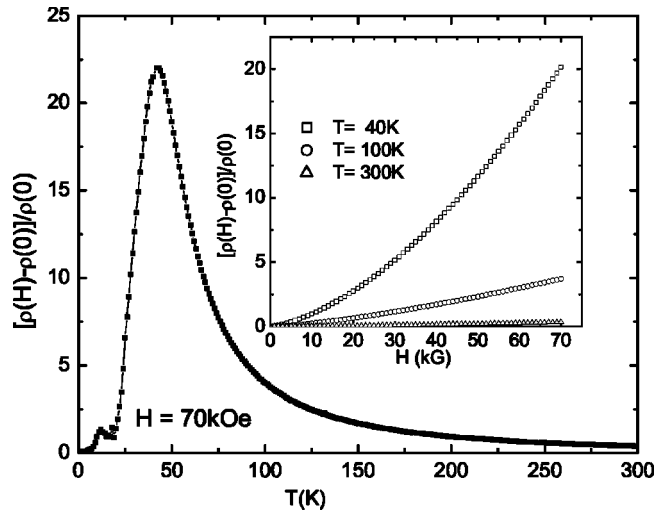


FIG. 5. Temperature dependent  $b$ -axis magnetoresistance. The inset shows magnetic isotherms around  $T_{\min}$  (40 K) and in the paramagnetic region (200 and 300 K).

with the activation energy of  $\Delta_p(b) \approx 250$  K [Fig. 4 (inset)]. Application of 70 kOe along the  $a$  and  $c$  axes has a small influence on resistivity ( $\Delta\rho/\rho < 0.15$ ), but, on the other hand, crossover temperature region in the  $b$ -axis resistivity disappears in this field.

It has been reported that  $\rho_{ab} > \rho_c$ .<sup>9</sup> Contrary to expected, we observed that high conductivity axis is not  $c$ , but the  $b$  axis. It should be noted that the observed metallic conductivity in the  $b$ -axis electrical transport as well as the  $T_{\min}$  are very sensitive to the current misalignment. The effect of a deliberate small misalignment in the current's path along the  $b$  axis in the  $ab$  plane is shown in Fig. 4 (approximate direction of current path and voltage pickup in a four-probe measurement has been slightly diverted from the  $b$  axis direction into the  $ab$  plane). RR above  $T_{\min}$  for sample 1 can be changed by a factor of 2 and  $T_{\min}$  can be shifted up 30 K in temperature.

As shown in Fig. 2, an applied field enhances  $b$ -axis resistivity near  $T_{\min}$  leading to a large magnetoresistance. The 70 kOe magnetoresistance is temperature dependant, and has a sharp maximum  $\Delta\rho/\rho = 22$  in the crossover region (Fig. 5). Magnetic isotherms [Fig. 5 (inset)] show  $H^\alpha$  dependence where  $\alpha = 1.5 - 1.7$ , a value smaller than  $\alpha = 2$  expected for a simple one-carrier system with an energy independent carrier relaxation time [ $\Delta\rho(H)/\rho_0 = \mu^2 H^2$  where  $\mu$  is the carrier mobility].

The marcasite-type FeSb<sub>2</sub> has been classified as a semi-metal or narrow gap semiconductor<sup>1,9</sup> in which both valence and conduction band are derived from  $d$ -like states.<sup>3,10</sup> We rationalize our observation of anisotropy in its physical properties within the framework of temperature induced transitions within the  $3d$  multiplet.

In the orthorhombic marcasite structure Fe (cation) is surrounded by a deformed Sb (anion) octahedra. These octahedra then share edges along the  $c$  axis (Fig. 1). The edge sharing octahedra form chains parallel to the  $c$  axis causing an overlap of the  $d_{xy}$  atomic orbitals. As opposed to normal marcasites with filled  $d_{xy}$  orbitals and a  $c/a$  ratio between

0.73–0.75, loellingites with  $d^2$  and  $d^4$  cations have a  $c/a$  ratio between 0.50–0.53 and empty  $d_{xy}$  orbital.<sup>1,2</sup> Based on the scheme given by Goodenough [see Fig. 2 (inset)],  $t_{2g}$  orbitals are further split into the two lower lying ( $\Lambda$ ) orbitals associated with  $d_{xz}$  and  $d_{yz}$ , and a higher lying ( $\Xi$ ) orbital associated with  $d_{xy}$  which create a  $\Xi$  band of itinerant electron states due to their overlap.<sup>3,11</sup> Starting at low temperatures, FeSb<sub>2</sub> is a diamagnetic semiconductor, as expected for  $S=0$  low spin  $d^4$  ground state ( $t_{2g}^4$ ,  $S=0$ ) where low energy  $\Lambda$  orbitals are filled with electrons with opposite spin due to crystalline fields which are larger than Hund's rule spin pairing energy.

We performed analysis of the thermal excitation from the ground state nonmagnetic ( $S=0$ ) to the paramagnetic excited ( $S \neq 0$ ) state: it results in a change of magnetic susceptibility

$$\chi(T) = Ng^2 \mu_B^2 \frac{J(J+1)}{3k_B T} \frac{2J+1}{2J+1 + \exp(\Delta_\chi/k_B T)},$$

where  $J=S$  and  $\Delta_\chi$  is the susceptibility gap.<sup>12</sup> A fit to the polycrystalline average of our data over entire temperature range for fixed  $g=2$  [Fig. 2 (inset)] describes well the behavior of FeSb<sub>2</sub> and yields  $\Delta_\chi \approx 546$  K,  $S=0.59$  for a spin value in the Curie constant and  $\chi_0 = -4 \times 10^{-5}$  (emu/mole). Diamagnetic anisotropy in the low spin state (see Fig. 2) is a consequence of the filled  $t_{2g}$  ground state orbitals. The magnetic susceptibility of FeSb<sub>2</sub> is reminiscent of the  $\chi(T)$  data seen in FeSi, albeit with diamagnetic susceptibility at low temperature and a much smaller tail below 5 K. The tail below 5 K (Fig. 2) corresponds to 0.5% of Fe<sup>2+</sup> impurities per mole, and the same impurity concentration is estimated from low temperature susceptibility measured in 10 kOe. Apart from the “free-ion-like” model of localized electrons described above, the model of metallic paramagnetism by Jaccarino *et al.* has been invoked to apply magnetic susceptibility of FeSi.<sup>4,12–14</sup> Attempts to interpret the magnetic susceptibility of FeSb<sub>2</sub> within this model of two narrow bands with rectangular and constant density of states of width  $W$  separated by energy gap  $E_g$  did not produce meaningful fitting parameters. However, since the magnetic moment seems to disappear along with the mobile carriers, a more refined analysis with a different band shape is necessary in order to make a definite statement about the validity of Jaccarino's model in this material. Moreover, since the difference in  $\Delta_\chi$  and  $\Delta_\rho$  seen in FeSi was explained in the framework of metallic paramagnetism by invoking the existence of an indirect (smaller) energy gap responsible for transport and a direct (larger) gap of the same width for both spin and charge excitations, possible Kondo-insulator-like features in FeSb<sub>2</sub> deserve further study.<sup>15</sup>

One possible explanation for the enhanced conductivity in a paramagnetic state and its anisotropy is the population of the  $\Xi$  band of itinerant states induced by thermal depairing on low energy  $\Lambda$  orbitals. As the temperature is raised, some of  $3d$  electrons are thermally excited to  $\Xi$  band responsible for conduction, while electrons in the localized  $\Lambda$  or  $e_g$  orbitals are responsible for temperature induced paramagnetic moment, as seen in magnetic susceptibility which shows a

significant enhancement above 100 K. Delocalization in this scenario is connected with a transition within the  $t_{2g}$  multiplet and it is possible that it occurs at lower temperatures than the transition to the higher lying  $e_g$  orbital which explains  $T_{\min}$  as low as 40 K for current applied along the  $b$  axis in diamagnetic state. We also note the difference between the susceptibility ( $\Delta_\chi$ ) and resistivity ( $\Delta_\rho$ ) gaps, indicating that the gap relevant for conductivity is smaller than the gap relevant for the susceptibility, an observation not in contradiction with above description. A possible difference between the gaps in charge and spin excitation channels has been also observed in some samples of FeSi.<sup>15</sup>

The large magnetoresistance (MR) seen in FeSb<sub>2</sub> for  $I\parallel b$  axis ( $\sim 2250\%$  at  $T_{\min}$  and  $\sim 32\%$  at  $T=300$  K in  $H=70$  kOe) is comparable in magnitude to the MR seen in giant magnetoresistance (GMR) materials such as manganate perovskites.<sup>16,17</sup> The spin disorder scattering mechanism of MR does not seem to be a viable mechanism in this material. One possible, but speculative, explanation of the large magnetoresistance phenomenon can be found in analogy with the extraordinary magnetoresistance (EMR) seen in non-magnetic semiconductors with embedded metallic inhomogeneities.<sup>18,19</sup> Since the  $\Xi$  band of conducting states is highly directional in real space, (our measurement in Fig. 3 also is consistent with this interpretation), it can act as a region of metallic conductivity in a semiconducting environment, short circuiting most of the applied current passing through it. In the simplest picture of isotropic conductivity, the single band carrier mobility is  $\mu=R_H\sigma$ . By including scattering time  $\tau$  through the general relation  $R_H=-\omega_c\tau/\sigma B$ , we obtain  $\mu B\sim\omega_c\tau$ . Large positive magnetoresistance is then a consequence of the large mobility of the carriers in the itinerant  $\Xi$  band since even modest fields could enhance the value of  $\omega_c\tau$ . The steep rise of the Hall

constant below 120 K seen in Ref. 7 holds the promise of reaching  $R_H\sim 10^{-1}$  cm<sup>3</sup>/C around  $T_{\min}=40$  K for the  $b$  axis resistivity. Taking  $\rho(T_{\min})\sim 50$   $\mu\Omega$  cm from our measurement, we estimate  $\mu(T_{\min})\sim 2000$  cm<sup>2</sup>/V s, comparable to the high mobility values found in antimony based materials with a skutterudite structure.<sup>20,21</sup> Hence, the condition  $H>1/\mu$  is satisfied for fields of the order of 50 kOe. Strong magnetoresistance therefore is likely to have its origin in band effects, and the above description is further supported with Kohler's rule  $\Delta\rho/\rho_0$  and  $H/\rho_0$  curves which fall on the single manifold (not shown) in the metallic region of the  $b$ -axis conductivity from 40 to 300 K. Measurement of the Hall coefficient at low temperature would be useful to clarify this issue as well as further crystallographic studies and band structure calculations for elucidating the orientation of the  $\Xi$  band. In addition, neutron scattering experiments could offer decisive information about thermally induced paramagnetism. Further study may explain physics contained in FeSb<sub>2</sub> in the single-electron picture, but on the other hand it might turn into a playground for many body effects in  $3d$  material with an anisotropic crystal and possible electronic structure. Since narrow gap semiconductors are important ingredients in optoelectronic devices for both civilian and military use, further study and tuning of FeSb<sub>2</sub> properties deserves some attention.

We thank Zachary Fisk, Vladimir Kogan, Maxim Dzero, Marcos Avila, Raquel Ribeiro, and Yongjae Lee for useful discussions. This work was carried out at Ames Laboratory, which is operated for the U.S. Department of Energy by Iowa State University under Contract No. W-7405-82. This work was supported by the Director for Energy Research, Office of Basic Energy Sciences of the U.S. Department of Energy.

\*Present address: Physics Department, Brookhaven National Laboratory, Upton, NY 11973.

<sup>1</sup>F. Hulliger, Nature (London) **198**, 1081 (1963).

<sup>2</sup>F. Hulliger, Struct. Bonding (Berlin) **4**, 83 (1967).

<sup>3</sup>J. B. Goodenough, J. Solid State Chem. **5**, 144 (1972).

<sup>4</sup>Z. Schlesinger, Z. Fisk, H-T Zhang, M. B. Maple, J. F. DiTusa, and G. Aeppli, Phys. Rev. Lett. **71**, 1748 (1993).

<sup>5</sup>Z. Fisk and J. P. Remeika, in *Handbook on the Physics and Chemistry of Rare Earths*, edited by K. A. Gschneidner and J. Eyring (Elsevier, Amsterdam, 1989), Vol. 12.

<sup>6</sup>P. C. Canfield and Z. Fisk, Philos. Mag. B **65**, 1117 (1992).

<sup>7</sup>P. C. Canfield and I. R. Fisher, J. Cryst. Growth **225**, 155 (2001).

<sup>8</sup>H. Holseth and A. Kjekshus, Acta Chem. Scand. **22**, 3273 (1968); A. Kjekshus and T. Rakke, Acta Chem. Scand., Ser. A **31A**, 517 (1977); T. Rosenqvist, Acta Metall. **4**, 761 (1953).

<sup>9</sup>A. K. L. Fan, G. H. Rosenthal, H. L. McKinze, and A. Wold, J. Solid State Chem. **5**, 131 (1972).

<sup>10</sup>C. E. T. Gonçalves da Silva, Solid State Commun. **33**, 63 (1980).

<sup>11</sup>In the labeling scheme given by Goodenough,  $\Lambda$  (Ref. 8) orbitals are labeled " $b$ ," and the higher lying  $\Xi$  orbital is labeled " $a_{\parallel}$ ."

We use different notation in order to avoid confusion with the crystalline axes orientation.

<sup>12</sup>V. Jaccarino, G. K. Wertheim, J. H. Wernick, L. R. Walker, and S. Aaraj, Phys. Rev. **160**, 476 (1967).

<sup>13</sup>G. K. Wertheim, V. Jaccarino, J. H. Wernick, J. A. Seitchik, H. J. Williams, and R. C. Sherwood, Phys. Lett. **18**, 89 (1965).

<sup>14</sup>D. Mandrus, J. L. Sarrao, A. Migliori, J. D. Thompson, and Z. Fisk, Phys. Rev. B **51**, 4763 (1995).

<sup>15</sup>S. Paschen, E. Felder, M. A. Chernikov, L. Degiorgi, H. Schwer, H. R. Ott, D. P. Young, J. L. Sarrao, and Z. Fisk, Phys. Rev. B **56**, 12 916 (1997).

<sup>16</sup>S. Lin, T. Tiefel, M. McCormack, R. Fastnacht, R. Ramesh, and L. Chen, Science **264**, 413 (1994).

<sup>17</sup>M. B. Salamon and M. Jaime, Rev. Mod. Phys. **73**, 583 (2001).

<sup>18</sup>T. Thio and S. A. Solin, Appl. Phys. Lett. **72**, 3497 (1998).

<sup>19</sup>Tineke Thio, S. A. Solin, J. W. Bennett, D. R. Hines, M. Kawano, N. Oda, and M. Sano, Phys. Rev. B **57**, 12 239 (1998).

<sup>20</sup>D. T. Morelli, T. Caillat, J. P. Fleurial, A. Borschevsky, J. Vandersande, B. Chen, and C. Uher, Phys. Rev. B **51**, 9622 (1995).

<sup>21</sup>NASA Technical Briefs, 60–61, March 1999.